RSC Advances

ROYAL SOCIETY OF CHEMISTRY

www.rsc.org/advances

RSC Advances

ARTICLE

Pyridine–Triazole Ligands for Copper–Catalyzed Aerobic Alcohol Oxidation

Pech Thongkam,[a,b] Sudarat Jindabot,[a,b] Samran Prabpai,[b] Palangpon Kongsaeree,[b] Taveechai Wittisuwannakul,[b] Panida Surawatanawong[b] and Preeyanuch Sangtrirutnugul[a,b]

A series of $[Cu(NN')]_2(OTf)_2$ complexes containing pyridine-triazole ligands [OTf = OSO_2CF_3; NN' = NN'_{Ph} (**1**), NN'_{hex} (**2**), NN'_{py} (**3**)] with different substituents at the triazole *N*4 position or 2,2'-bipyridine (bpy; **4**) have been synthesized. Crystal structures of **1** and **3** reveal a *trans*-isomer with strong preference for regular-type triazole coordination (for **3**) whereas the Cu-bipyridine complex **4** is more stable in a *cis*-form. Cyclic voltammetry of **1**–**4** suggest that the electron-donating strength follows the trend: bpy > NN'_{py} > NN'_{hex} ~ NN'_{Ph}. The catalyst systems consisting of 5 mol% $CuOTf_2$/NN'/TEMPO (TEMPO = (2,2,6,6-tetramethylpiperidin-1-yl)oxy) in the presence of 2x2.0 cm^2 Cu^0 sheets as a reducing agent and 10 mol% *N*-methylimidazole (NMI) exhibit good activities for aerobic oxidation of benzyl alcohol to benzaldehyde. Catalytic studies have shown that the activities were higher with more electron-rich N-based ligands. Furthermore, oxidation of aliphatic alcohols such as 1-hexanol and 2-methyl-1-pentanol using the Cu catalyst system with the NN'_{py} ligand at room temperature afforded the corresponding aldehydes in >99% and 46% yields, respectively after 24 h.

Received 00th January 20xx,
Accepted 00th January 20xx

DOI: 10.1039/x0xx00000x

www.rsc.org/rscadv

1. Introduction

Oxidation of alcohols to aldehydes is one of the most important classes of organic transformation.[1, 2] Classical alcohol oxidation reactions to aldehydes usually employ stoichiometric amounts of strong oxidants such as chromium(VI) oxide-pyridine,[3] oxalylchloride/DMSO,[4] Dess-Martin periodinane (DMP),[5] and NaOCl/TEMPO (TEMPO = (2,2,6,6-tetramethylpiperidin-1-yl)oxy).[6] Thus, an improvement toward greener and more economical synthetic alternatives including the use of molecular oxygen as a primary oxidant and recyclable metal catalysts is needed. Up to now, various types of transition metal catalysts such as vanadium, cobalt, and molybdenum have been employed in aerobic alcohol oxidation.[7] In particular, copper complexes have attracted considerable attentions since copper species are found in active sites of several oxidase enzymes, which are known to catalyze aerobic oxidation reactions under mild conditions.[8-10] In 1984, Semmelhack and co-workers reported effective alcohol oxidation catalyzed by $Cu^{I}Cl$/TEMPO in the presence of O_2 gas.[11] Markó *et. al.* later demonstrated that CuCl(Phen–$DEADH_2$) (Phen 1,10-phenanthroline; $DEADH_2$ = diethylhydrazinodicarboxylate) was efficient at the oxidation of 1^o and 2^o alcohols under 1 atm of O_2 at 90 °C.[12, 13] Sheldon also reported oxidation of 1^o alcohols catalyzed by $CuBr_2$(bpy) (bpy = 2,2'-bipyridine), TEMPO, and KO^tBu in a 2:1 mixture of CH_3CN:H_2O under air at room temperature.[14] By replacing KO^tBu with organic base, Koskinen has shown that the catalyst system CuX_2(bpy)/TEMPO/base [X = Br or OTf; base = *N*-methylimidazole (NMI) or 1,8-diazabicycloundec-7-ene (DBU)] could efficiently catalyze benzylic and allylic alcohol oxidation under mild conditions.[15] More recently, Stahl and co-workers reported that the catalyst system $Cu^{I}OTf$/bpy/NMI in CH_3CN exhibited better oxidation performance compared to its Cu^{II} analogue and, based on kinetic and spectroscopic studies, the mechanism of Cu^{I}/TEMPO-catalyzed alcohol oxidation has been proposed (Scheme 1).[16-18] In addition, the effect of bpy ligand on redox potentials at copper center and consequently catalytic activities toward alcohol oxidations has been studied.[17]

Over the past decade, 1,2,3-triazole ("click") compounds have been widely used in applications including polymer,[19] material research,[20] and catalysis mainly due to ease of preparation and structural modification. For catalytic application, reported organic reactions mediated by transition metal complexes featuring 1,2,3-triazole ligands are, for example, alkyne-azide cycloaddition,[21] polymerization,[19, 22, 23] C–C coupling,[24-26] epoxidation,[27] and propargyl alcohol dehydration.[28] In comparison to pyridine, the electronically similar 1,2,3-triazole compounds are aromatic with better π accepting ability, based on photophysical and electrochemical studies of the Ru(II) complexes.[29]

[a] Center for Catalysis, Department of Chemistry, Faculty of Science, Mahidol University, 272 Rama VI Rd., Bangkok 10400, Thailand.
[b] Department of Chemistry and Center of Excellence for Innovation in Chemistry, Faculty of Science, Mahidol University, 272 Rama VI Rd., Bangkok 10400, Thailand.

† Electronic Supplementary Information (ESI) available: Supplementary UV–vis spectra, DFT calculations, and CIFs providing crystallographic data for **1**•$2H_2O$, **3**, and **4**. See DOI: 10.1039/x0xx00000x

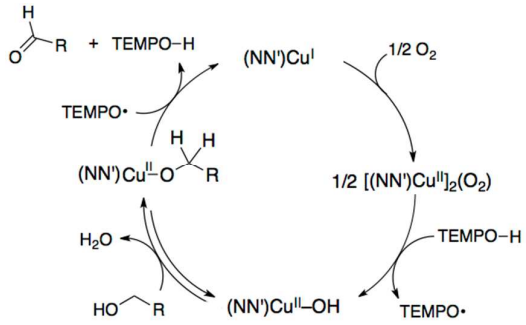

Scheme 1. Catalytic mechanism for Cu^{I}/TEMPO-catalyzed aerobic alcohol oxidation.

Another interesting feature of 1,2,3-triazole compounds is that the substituents at the 1- and 4-positions can be conveniently adjusted and this facilitates the study of ligand substituent effect. In this work, we investigated a series of pyridine-triazole ligands, related to the more well known bidentate N-based ligand 2,2'-bipyridine, for copper-catalyzed alcohol oxidation. The use of oxidatively more stable Cu(II) complexes in the presence of a reducing agent Cu^{0} to generate the catalytically active Cu(I) species *in situ* was also explored. In addition, the effect of substituents at the 1,2,3-triazole ring and triazole configurations on redox potentials at the copper center and catalytic oxidation activities were studied.

2. Results and discussion

2.1 Synthesis and characterization

A series of bidentate pyridine-triazole ligands of the type 2-(4-R-1,2,3-triazol-1-yl)pyridine [R = C_6H_5 (NN'$_{Ph}$), *n*-C_6H_{13} (NN'$_{hex}$), NC_5H_4 (NN'$_{py}$)] were prepared following those reported in the literature (Figure 1).[24] Reactions of Cu(OTf)$_2$ and 2.1 equiv of the pyridine-triazole ligands in either a mixture of CH_3CN/CH_2Cl_2 or CH_3CN at room temperature afforded the corresponding, distorted octahedral Cu(II) complexes Cu(NN')$_2$(OTf)$_2$ [NN' = NN'$_{Ph}$ (**1**), NN'$_{hex}$ (**2**), NN'$_{py}$ (**3**)] in good yields (81–83% yields). For comparison, the analogous Cu(bpy)$_2$(OTf)$_2$ was also prepared under similar reaction conditions, giving blue crystalline solids as the product **4** in 87% yield. The resulting Cu(II) complexes **1**–**4** were isolated via crystallization from the CH_3CN solution and characterized by UV-vis spectroscopy (Figure S4–7, ESI), single-crystal X-ray diffraction (XRD) studies (for **1**, **3**, and **4**), powder XRD (for **3** and **4**, Figure S8, ESI), and elemental analysis.

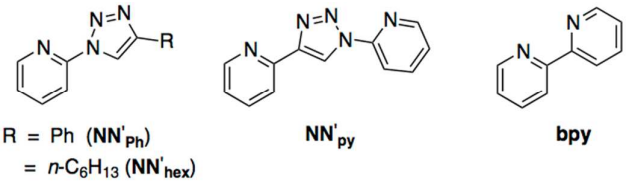

Figure 1. Structures of the ligands NN'$_{Ph}$, NN'$_{hex}$, NN'$_{py}$, and bpy

2.2 Description of crystal structures

The solid state structures of **1** and **3** reveal distorted octahedral geometry with two bidentate NN' ligands and inner-sphere triflate ions bound to the Cu(II) center in a *trans* stereoisomer (Figure 2). Furthermore, for both complexes **1** and **3**, the pyridyl N and the triazole N donors are mutually *trans* to each other. This structural arrangement has previously been observed in related octahedral *bis*(pyridine-triazolyl) complexes of Cu(II),[30] Ni(II),[31] and Zn(II)[32] as well as square planar Pd(II) complexes.[33]

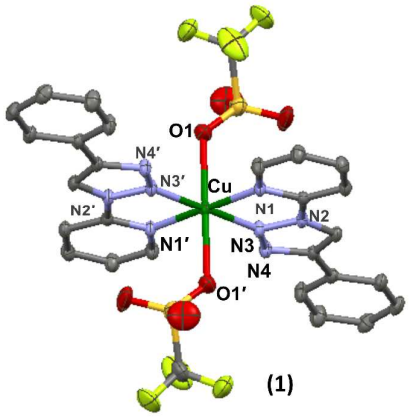

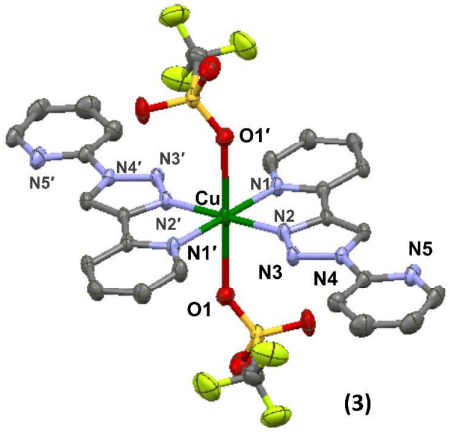

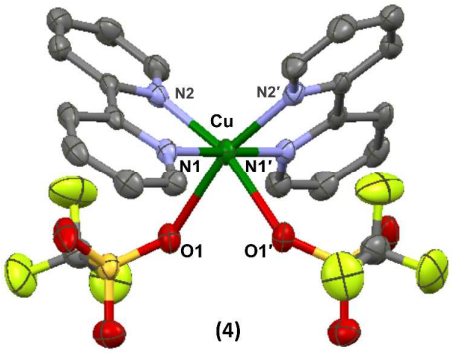

Figure 2. ORTEP representations of complexes **1** (left), **3** (right), and **4** (middle) showing 30% probability displacement ellipsoids and partial atom-labeling scheme. Hydrogen atoms and water molecules (for **1**) were omitted for clarity.

Table 1. Selected bond lengths (Å).

	1	**3**	**4**
Cu–N(py)	2.024(2)	2.054(2)	1.970(3), 2.075(3)
Cu–N(trz)	1.980(2)	1.992(2)	-
Cu–O(1)	2.424(3)	2.394(2)	2.403(3)

Table 2. Selected bond angles (°).

	1	**3**	**4**
N(py)–Cu–N(py)	180.0	180.0	80.70(13)[a]
N(py)–Cu–N(trz)	79.98(10)[a]	80.77(7)[a]	-
N(trz)–Cu–O1	91.04(10)	91.93(7)	-
N(py)–Cu–O1	87.89(10)	84.60(7)	92.44(12) (*cis*) 164.57(11) (*trans*)

[a] Bite angle

For complex **3**, due to the more electron rich nature, the proximal triazole N donor (*N*2) or the 2-(1*H*-1,2,3-triazol-4-yl)pyridine chelate pocket (*i.e.*, regular-type triazole ligand) exclusively binds to Cu(II) instead of the medial triazole N (*N*3), as shown in Figure 2. The selective formation of the regular triazole complexes has been previously observed with the related Pd(II) compound $(NN'_{py})PdCl_2$[24] and by ligand exchange experiments reported by Crowley and co-workers.[34] In general, the Cu–N bond lengths of **1** are marginally shorter than those of **3** while the bond distances of Cu–N(py) and Cu–N(trz) are within the expected ranges compared to similar Cu^{II} complexes supported by pyridine-triazole ligands [*i.e.*, 2.003–2.062 Å for Cu–N(py) and 1.985–2.037 Å for Cu–N(trz)],[30] with slightly shorter Cu–N(trz) bonds compared to Cu–N(py) (Table 1). In contrast to **1** and **3**, the solid state structure of $Cu(bpy)_2(OTf)_2$ (**4**; Figure 2) shows a *cis* isomer, where both triflate ions are located *trans* to pyridyl N donors. For all complexes, ligand bite angles are in the range of *ca.* 80.0°–80.8° (Table 2). The purity of the representative crystalline complexes **3** and **4** in bulk phase was confirmed by powder X-ray diffraction (XRD) data compared to the simulative patterns (Figure S8, ESI).

2.3 Electronic spectra and electrochemical properties

The profiles of UV-visible spectra of **1**–**4** in CH_3CN appear similar (Supporting Information Figures S4–S7). Broad low-intensity bands at λ_{max} = 678, 664, 657, and 733 nm (for **1**–**4**, respectively) are assigned to the low-energy *d*-*d* transitions of the Cu(II) center. Since the *d*-*d* band shifts are associated with ligand field strength, the blue-shifted *d*-*d* transitions indicate stronger ligand fields, giving the order of ligand field factor as follows: $NN'_{py} > NN'_{hex} > NN'_{Ph} >$ bpy.

The electrochemical properties of complexes **1**–**4** were investigated by cyclic voltammetry (CV) using dry CH_3CN solvent under Ar (Figure 3) and the CV data were summarized in Table 3. Complexes **1** and **2** featuring NN'_{Ph} and NN'_{hex} ligands exhibit similar quasi-reversible redox waves with cathodic reductions corresponding to the Cu(II)/Cu(I) couple (Ep_c) at –0.050 and –0.070 V and slightly weaker anodic responses (Ep_a) at 0.373 and 0.323 V, respectively (Table 3). For complex **3** with regular-type triazole binding to Cu(II), there is a significant negative shift of the reduction potential (Ep_c = –0.473 V) and unexpectedly weak Cu(I)→Cu(II) oxidation wave, suggesting the Cu(I) species supported by NN'_{py} is relatively unstable. However, at scan rate 100 mV s^{-1}, no anodic stripping of copper, a result of the Cu(I)/Cu(0) couple, is observed.[10, 35, 36] In addition, of all complexes, **4** possesses the most negative reduction potential with Ep_c = –0.666 V. It is worth mentioning that Stahl and co-workers previously reported the Cu(II)/Cu(I) reduction potential of –0.18 V for an CH_3CN solution mixture of $[Cu^{I}(CH_3CN)_4]OTf$ and 4 equiv of bpy.[16] Since the more negative reduction potentials assignable to Cu(II)→Cu(I) are attributed to higher electron density at the copper center and consequently the electron-donating ability of ligands, the electron-donating property decreases following the trend: bpy > NN'_{py} > NN'_{hex} ~ NN'_{Ph}.

Although, based on the reduction potentials, bpy appears to be the most electron-donating ligand for the Cu(II) complexes of the type $Cu(NN')_2(OTf)_2$, we cannot ignore the difference in stereoisomers, which may also influence the observed redox potentials.[37]

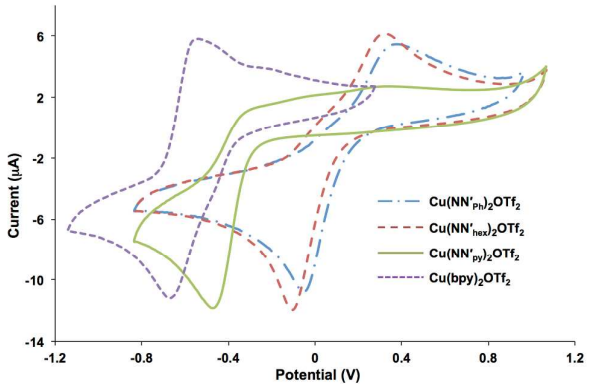

Figure 3. Overlaid cyclic voltammograms of **1**–**4** in CH_3CN solution. Scan rate 100 mV s^{-1}.

Table 3. Cyclic Voltammetry Analysis of $Cu(NN')_2OTf_2$ complexes[a]

Complex	E_{ox} [V]	E_{red} [V]	ΔE_p [mV]	$E_{1/2}$[b] [V]
1	0.373	–0.050	423	0.162
2	0.323	–0.070	393	0.126
3		–0.473		
4	–0.537	–0.666	129	–0.601

[a] Conditions: 1 mM $Cu(NN')_2OTf_2$, in CH_3CN, 0.1 M $[NEt_4][PF_6]$, glassy carbon working electrode, platinum counter electrode, Ag/Ag^+ reference electrode, scan rate 100 mV/s, potentials reported in relative to Fc/Fc^+. [b] $E_{1/2} = (E_{p,a} + E_{p,c})/2$.

Interestingly, the complex **2** with a saturated and electron-donating hexyl substituted NN'_{hex} ligand resulted in only slightly more cathodic shift by –20 mV compared to that of **1**, containing an aromatic phenyl substituent. This small potential difference suggests that the type of substituents at the triazole *N*4 position have little effect on the electron density at the copper center.[29, 38] On the other hand, triazole configurations involving chelation through regular-type or inverse-type triazole N donor exert more impact on the electron density at copper. In particular, the regular-type triazole ligand using proximal triazole N donor affords more electron-rich copper center than the inverse-type triazole ligand.

2.4 DFT calculation

Since the triazole chelation through inverse-type (in **1**) *vs*. regular-type (in **3**) configurations can affect the electron donating ability of the ligands and activity for alcohol oxidation of the catalysts, we performed density functional calculations to gain insights into the electronic structures related to the redox properties of **1** and **3**. Generally, Cu(I) complex often favors a tetrahedral geometry, as evidenced by previously reported crystal structures of Cu(I) complexes with bidentate N-donor ligands including $[Cu(bpy)_2]ClO_4$[39] and $[Cu(phen)_2]ClO_4$.[40] Our calculated structure of $[Cu(bpy)_2]^+$ is in good agreement with the available crystal structures (Supporting Information Table S2). Here, the reduced species of **1** and **3** are calculated as tetrahedral complexes, $[Cu(NN'_{Ph})_2]^+$ and $[Cu(NN'_{py})_2]^+$ (Figure 4), consistent with the previously reported tetrahedral structure of the related Cu(I) complex $[Cu(\mathbf{L})_2]\bullet BF_4$ (**L** = 2-(1-benzyl-1,2,3-triazol-4-yl)pyridine). Similar to their corresponding Cu(II) complexes, these Cu(I) complexes display slightly shorter Cu–N(trz) bonds compared to the Cu–N(py) bonds.

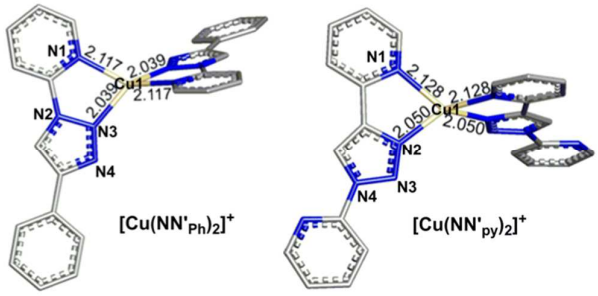

APT Charge	$[Cu(NN'_{Ph})_2]^+$	$[Cu(NN'_{py})_2]^+$
Cu1	0.591	0.556
N1	–0.385	–0.337
N2	–0.541	–0.139
N3	0.065	0.024
N4	–0.319	–0.537

Figure 4. Optimized geometries of $[Cu(NN'_{Ph})_2]^+$and $[Cu(NN'_{py})_2]^+$ (the reduced forms of **1** and **3**, respectively) with APT charges shown on selected atoms. Calculated bond distances are given in Å. All H atoms are omitted for clarity. Cu atoms are shown in white, C atoms in grey, and N atoms in blue.

Molecular orbitals (MOs) and MO energies of $[Cu(NN'_{Ph})_2]^+$ and $[Cu(NN'_{py})_2]^+$ show that all five metal *d*-based orbitals are occupied (Figure 5) representing d^{10} configuration. Although both complexes have HOMO with a σ-antibonding interaction between the Cu d_{xz} and the NN' ligands, the HOMO energy of $[Cu(NN'_{py})_2]^+$ is relatively higher than that of $[Cu(NN'_{Ph})_2]^+$. Thus, one-electron reduction of **3** to form its reduced complex $[Cu(NN'_{py})_2]^+$ is expected to be less favored than the same process of **1** to form $[Cu(NN'_{Ph})_2]^+$. Using the same reasoning, O_2 activation by Cu(I) catalysts to afford the corresponding Cu(II) superoxo species, proposed as turnover-limiting step for activated benzyl alcohol substrates,[17, 18] should occur more readily with $[Cu(NN'_{py})_2]^+$. This result is also in agreement with the observed reduction potentials, which are more negative for complex **3** relative to **1**. Moreover, the APT charges on *N*2 and *N*4 of the triazole are rather negative while the charge on

*N*3 is almost neutral for both $[Cu(NN'_{Ph})_2]^+$ and $[Cu(NN'_{py})_2]^+$ (Figure 4). Therefore, the regular-type binding mode of the triazole should lead to a stronger ligand σ-donation in $[Cu(NN'_{py})_2]^+$ and potentially the more active alcohol oxidation catalyst.

2.5 Catalytic test for aerobic alcohol oxidation

To optimize reaction conditions, benzyl alcohol was chosen as a model substrate for copper-catalyzed alcohol oxidation. A mixture of $Cu(OTf)_2$ (5 mol%), Cu^0 sheet (4.0 cm^2), *N*-methylimidazole (NMI, 10 mol%), and NN' ligand (5 mol%) was used as the catalyst system in the presence of TEMPO (5 mol%) radical. The reactions were carried out at room temperature in CH_3CN under aerobic conditions. In a typical experiment, after a given time, the product in the reaction mixture was analyzed using GC-MS. In general, the reaction gave good to excellent yields of benzaldehyde after 3 h, with no over-oxidized benzoic acid observed (Table 4, entries 1–4). Complete conversions to benzaldehyde were observed with NN'_{py} and bpy ligands while the catalyst systems containing NN'_{Ph} and NN'_{hex} ligands afforded the product in 77% and 80% yields, respectively. Based on its high activity, the molecular complex $Cu(NN'_{py})_2(OTf)_2$ (**3**) and Cu^0 was investigated as a catalyst under the same reaction conditions and found that the catalytic oxidation of **3**/Cu^0 was only slightly faster than that of the system $Cu(OTf)_2/NN'_{py}/Cu^0$, giving 86% and 73% product yields, respectively, after 2 h (entries 5 and 3). Since we expected reduction of Cu^{II} species by Cu^0 to generate the active Cu^I catalyst, a controlled reactions were carried out in the absence of Cu^0 (entry 6) and $Cu(OTf)_2$ (entry 7), both of which gave a lower product yields (22% and 66% after 24 h, respectively). In addition, even though reduced catalyst loadings of $Cu(OTf)_2/NN'_{py}$ gave slower conversions (Table 4, entries 8–10), the high percentage yield of 87% was still obtained with 0.05 mol% of $Cu(OTf)_2/NN'_{py}$ after 24 h.

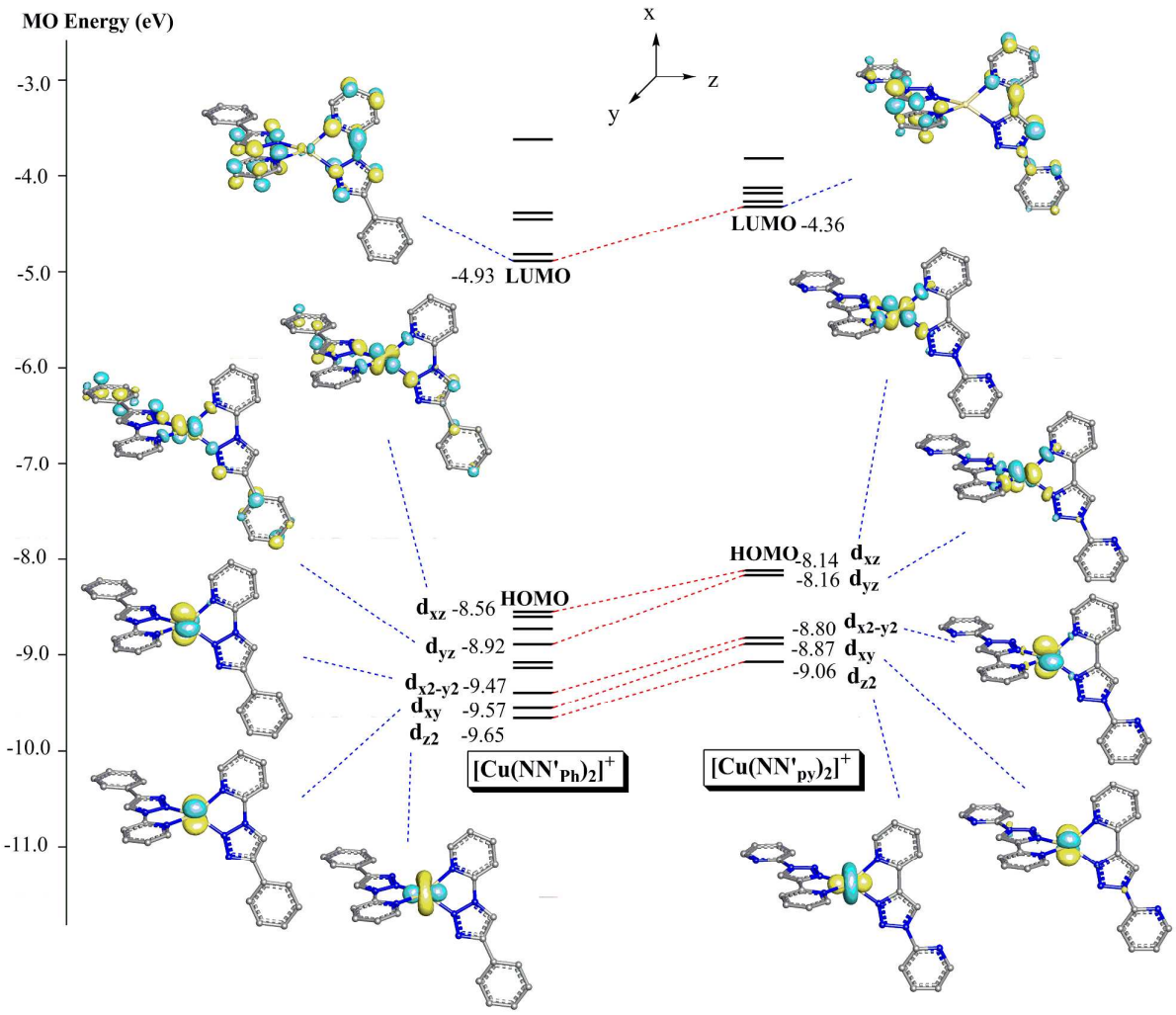

Figure 5. Calculated molecular orbitals (MOs) and MO energies (in eV) of $[Cu(NN'_{Ph})_2]^+$ and $[Cu(NN'_{py})_2]^+$.

Other substituted benzyl alcohols were also used as substrates and the oxidation results showed that all of them gave excellent and selective conversions to the corresponding aldehydes (entries 11–14). The non-activated aliphatic alcohol 1-hexanol could also be quantitatively converted to hexanal after 24 h although the more sterically hindered 2-methyl-1-pentanol resulted in a lower yield under the same conditions (entries 15 and 16). Noted that for secondary alcohols, no oxidation of cyclohexanol to cyclohexanone was observed whereas the more reactive 2-cyclohexen-1-ol was oxidized at room temperature to afford the corresponding ketone product in 55% yield after 24 h, based on GC-MS (entries 17 and 18).

To evaluate the effect of N-based ligands NN' and bpy on the catalyst activities, the reaction mixtures from entries 1–4 (Table 4) were sampled and percent formation of the benzaldehyde product was monitored over time using GC-MS (Figure 6). The results showed the fastest initial conversion of benzyl alcohol oxidation for the catalyst system $Cu(OTf)_2$/bpy/Cu^0. In general, the catalytic activity follows the order: bpy > NN'_{py} > NN'_{hex} ~ NN'_{Ph}. This observed activity trend is consistent with the ligand electron-donating ability, based on the CV results (*vide supra*). In other words, more electron-rich ligands resulted in more active copper catalyst systems for oxidation. Along the same line, Stahl and co-workers have recently observed that reaction rates of copper-catalyzed aerobic alcohol oxidation were higher with 4,4'-dimethoxy-2,2'-bipyridine ligand compared to 2,2'-bipyridine.[41] In addition, previous catalyst screenings reported by Repo and co-workers have shown that rigid and strongly coordinating ligands generally afforded more active copper catalysts for oxidation of benzyl alcohol in alkaline-water solutions at 80 °C under 10 bar of O_2.[42] Reusability studies of the catalyst system $Cu(OTf)_2/NN'_{py}/Cu^0$ were also evaluated. It was found that the copper catalysts with added benzyl alcohol substrate and 5 mol% TEMPO remained effective giving >98% conversion for at least five reaction cycles without a loss in catalytic activities (Figure 7).

Table 4. Aerobic Oxidation of selected alcohols[a]

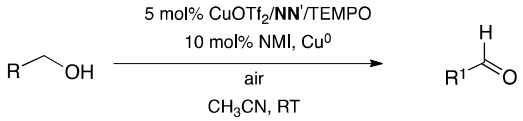

Entry	Cu source	Ligand	Substrate	Product	Time (h)	Yield (%)[b]
1	$Cu(OTf)_2/Cu^0$	NN'_{Ph}	Benzyl alcohol	Benzaldehyde	3	77
2	$Cu(OTf)_2/Cu^0$	NN'_{hex}	Benzyl alcohol	Benzaldehyde	3	80
3	$Cu(OTf)_2/Cu^0$	NN'_{py}	Benzyl alcohol	Benzaldehyde	3	>99 (73)[c]
4	$Cu(OTf)_2/Cu^0$	bpy	Benzyl alcohol	Benzaldehyde	3	>99
5	**3**/Cu^0	-	Benzyl alcohol	Benzaldehyde	3	98 (86)[c]
6[d]	**3**	-	Benzyl alcohol	Benzaldehyde	24	22
7[e]	Cu^0	NN'_{py}	Benzyl alcohol	Benzaldehyde	24	66
8[f]	$Cu(OTf)_2/Cu^0$	NN'_{py}	Benzyl alcohol	Benzaldehyde	24	>99
9[g]	$Cu(OTf)_2/Cu^0$	NN'_{py}	Benzyl alcohol	Benzaldehyde	24	92
10[h]	$Cu(OTf)_2/Cu^0$	NN'_{py}	Benzyl alcohol	Benzaldehyde	24	87
11	$Cu(OTf)_2/Cu^0$	NN'_{py}	4-MeO-benzyl alcohol	4-MeO-benzaldehyde	2	95 (>99)[i]
12	$Cu(OTf)_2/Cu^0$	NN'_{py}	4-NO_2-benzyl alcohol	4-NO_2-benzaldehyde	2	>99
13	$Cu(OTf)_2/Cu^0$	NN'_{py}	2-MeO-benzyl alcohol	2-MeO-benzaldehyde	2	82 (>99)[j]
14	$Cu(OTf)_2/Cu^0$	NN'_{py}	2-NO_2-benzyl alcohol	2-NO_2-benzaldehyde	2	67 (>99)[j]
15	$Cu(OTf)_2/Cu^0$	NN'_{py}	1-Hexanol	Hexanal	24	99
16	$Cu(OTf)_2/Cu^0$	NN'_{py}	2-Methyl-1-pentanol	2-Methylpentanal	24	46
17	$Cu(OTf)_2/Cu^0$	NN'_{py}	Cyclohexanol	Cyclohexanone	24	0
18	$Cu(OTf)_2/Cu^0$	NN'_{py}	2-Cyclohexen-1-ol	2-Cyclohexen-1-one	24	55

[a] Typical Conditions: 2.0 mmol of the substrate, 0.10 mmol (5 mol%) of $Cu(OTf)_2$/Ligand, 0.10 mmol (5 mol%) of TEMPO, 0.20 mmol (10 mol%) of NMI, 8 Cu^0 sheets (0.4 cm^2/mL) in CH_3CN (10 mL), 1 atm of air. [b] % yield was obtained based on GC analyses. [c] yields obtained after 2 h. [d] In the absence of Cu^0 sheet. [e] In the absence of $Cu(OTf)_2$. [f] 1 mol% of $CuOTf_2/NN'_{py}$. [g] 0.1 mol% of $CuOTf_2/NN'_{py}$. [h] 0.01 mol% of $CuOTf_2/NN'_{py}$. [i] yields obtained after 3 h. [j] yields obtained after 4 h.

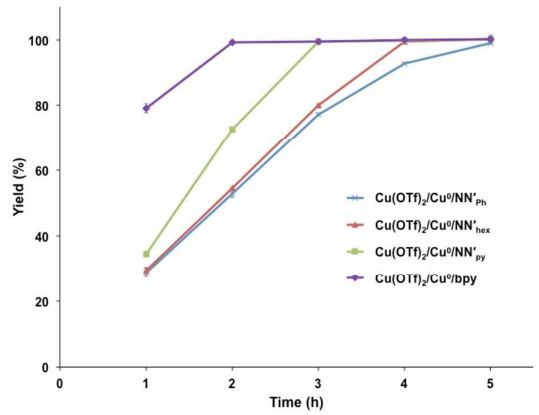

Figure 6. Percentage of benzaldehyde product *vs*. time

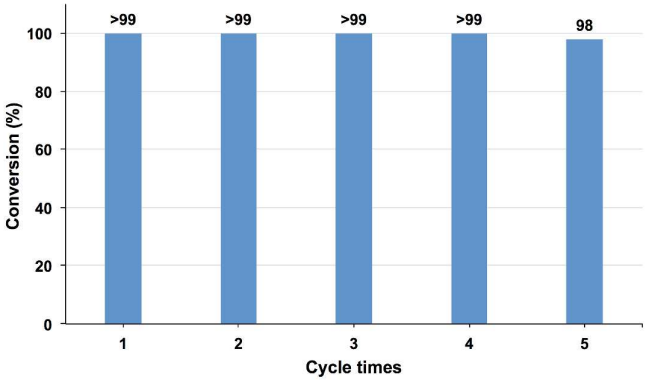

Figure 7. Reusability tests based on percent benzyl alcohol conversions over five reaction cycles

3. Experimental

3.1 General procedure

Air-sensitive syntheses were carried out under Ar using standard Schlenk techniques or in a Braun drybox. Toluene (Fisher Scientific) was dried using PURE SOLV MD-5 solvent purification system from Innovative Technology Inc. All other solvents were used as received. $(CuOTf)_2 \bullet C_6H_6$ (Aldrich) was used as received and stored under Ar. $Cu(OTf)_2$, 2-bromopyridine, phenylacetylene, 2-ethynylpyridine, *N*-methylimidazole (NMI), benzyl alcohol, other alcohol substrates, and 2,2'-bipyridine were purchased from Aldrich and used without further purification. Ethylenediaminetetraacetic acid (EDTA; LobaChemie), 1-octyne (Merck), anisole (Merck), 1-hexanol (Fluka), 2,2,6,6-tetramethylpiperidin-1-yl)oxy (TEMPO; Acros Organics) were also used as received. 2-azidopyridine and 2-(4-R-1,2,3-triazol-1-yl)pyridine [R = C_6H_5 (NN'_{Ph}), *n*-C_6H_{13} (NN'_{hex}), NC_5H_4 (NN'_{py})] were prepared according to the literature.[24]

^{1}H (500.1 MHz) NMR spectra were acquired on Bruker AV-500 spectrometer equipped with a 5 mm proton/BBI probe at room temperature and referenced to protic impurities in the deuterated solvent. Elemental analyses were conducted at Chemistry department, Mahidol University. Product yields and percent substrate conversions obtained from catalytic experiments were analyzed by GLC on a 6890N Agilent Technologies gas chromatograph equipped with a 5973N Agilent Technologies quadrupole mass detector. UV-vis spectra of the CH_3CN solutions (0.03 mM and 1 mM) were collected using a Jasco Model V-530 UV-vis spectrophotometer. Powder X-ray diffraction (XRD) measurements were collected using Bruker D8 ADVANCE diffractometer (Cu Kα radiation with Ge-crystal (Johansson type) monochromator (λ = 0.15406 nm)).

3.2 Synthesis and characterization

3.2.1 Synthesis of Cu(II) Complexes 1, 3, and 4. To a stirring 5 mL of CH_3CN solution of $Cu(OTf)_2$ (0.45 mmol) was added a 5 mL CH_2Cl_2 solution of NN' ligand (0.90 mmol) at room temperature. After 4 h, the reaction mixture was filtered and the precipitates were washed with 20 mL of CH_2Cl_2.

***trans*-Cu(NN'_{Ph})$_2$(OTf)$_2$ (1).** The product was obtained as a light green solid in 81% yield (0.29 g, 0.36 mmol). Anal. Calcd. for $C_{28}H_{20}N_8CuF_6O_6S_2$: C, 41.72; H, 2.50; N, 13.90. Found: C, 41.67; H, 2.30; N, 14.21.

***trans*-Cu(NN'_{py})$_2$(OTf)$_2$ (3).** The product was obtained as a blue solid in 83% yield (0.30 g, 0.37 mmol). Anal. Calcd. for $C_{26}H_{18}N_{10}CuF_6O_6S_2$: C, 38.64; H, 2.25; N, 17.33. Found: C, 39.02; H, 2.39; N, 17.70.

***cis*-Cu(bpy)$_2$(OTf)$_2$ (4).** The product was obtained as a blue solid in 87% yield (0.26 g, 0.39 mmol). Anal. Calcd. for$C_{22}H_{16}N_4CuF_6O_6S_2$: C, 39.20; H, 2.39; N, 8.31. Found: C, 39.33; H, 2.41; N, 8.28.

3.2.2 Synthesis of *trans*-Cu(NN'_{hex})$_2$(OTf)$_2$ (2). To a stirring 30 mLCH_3CN solution of $Cu(OTf)_2$ (0.53 g, 1.46 mmol) was added a 20 mL CH_3CN solution of NN'_{hex} (0.67 g, 2.91 mmol) at room temperature. After 5 h, the solvent was removed under vacuum. The remaining solid was purified by crystallization in CH_3CN at 0 °C to afford **2**, as a blue crystalline solid in 81% yield (0.97 g, 1.18mmol). Anal. Calcd. for $C_{28}H_{36}N_8CuF_6O_6S_2$: C, 40.90; H, 4.41; N, 13.63. Found: C, 40.70; H, 4.39; N, 13.71.

3.3. Cyclic voltammetry

Voltammograms were recorded at ambient temperatures with μAutolab Type III potentiostat and NOVA software. The Cu(II) complexes $Cu(NN')_2(OTf)_2$ (1.0 mM) was dissolved in dry CH_3CN containing 0.1 M $[Et_4N][PF_6]$ electrolyte. Measurements were performed under Ar at a scanning rate of 0.1 V s^{-1} with a glassy carbon working electrode, a platinum counter electrode, and a Ag/Ag^+ reference electrode. The sample was referenced to the ferrocene internal standard and its potentials were reported *versus* those of Fc/Fc^+.

3.4. X-ray analysis

Crystals of **1**, **3**, and **4** were grown from slow evaporation of the CH_3CN solution of the corresponding Cu(II) complexes at room

temperature. The single crystal X-ray analyses of Cu(II) complexes **1**, **3**, and **4** were carried out at the Mahidol Crystallographic Facility. Diffraction measurements were recorded using a 4 K Bruker APEX CCD area detector diffractometer with graphite-monochromated Mo *Kα* radiation (λ = 0.71073 Å). The structures were solved by the SHELX[43] or OLEX2[44] crystallographic software packages, using direct methods (SIR97)[45] and refined by full-matrix least-squares method on $(F_{obs})^2$ using the SHELXL97[46] software package. Complexes **1**•2H_2O and **3** crystallize in the orthorhombic system, space group *P*cba, and the triclinic system, space group *P*-1, respectively. In addition, both complexes **1**•2H_2O and **3** show the Cu atom in a centrosymmetric position whereas the complex**4**, in the *C*2/*c* space group, has the Cu atom on a 2-fold axis. All non-hydrogen atoms were refined anisotropically while the hydrogen atoms were included in calculated positions and refined as riding atoms with individual isotropic displacement parameters. Crystallographic data of **1**•2H_2O, **3**, and **4** are listed in Supporting Information Table S1.

3.5. Computational detail

All calculations were performed with the Gaussian 09 program.[47] All structures were fully optimized using B3LYP[48-50] density functional with default convergence criteria and frequencies were calculated to ensure that there is no imaginary frequency for minima. The Stuttgart relativistic small core (RSC)[51] 1997 ECP basis set was used for Cu and 6-31++G(d,p)[52-54] for all other atoms. Molecular orbitals were plotted by Jimp2 visualizing program.[55-57]

3.6. General procedures for Cu-catalyzed aerobic alcohol oxidation

2.0 mmol of alcohol was added into a 2 mL CH_3CN solution of $Cu(OTf)_2$ (0.10 mmol), followed by addition of Cu^0 sheets (total surface area = 4.0 cm^2). The reaction mixture was stirred for 10 min. Then, a 5 mL CH_3CN solution of NN' (0.10 mmol) was added into the reaction mixture, followed by addition of a 3 mL CH_3CN solution of TEMPO (0.10 mmol) and NMI (0.20 mmol). The reaction solution was allowed to stir at room temperature for a given time, after which it was filtered through a silica column using ethyl acetate as eluent. The product yields were determined using GC-MS methods with anisole (0.20 mmol) as an internal standard. For kinetic studies, the reaction solution was sampled for GC-MS analysis every hour for 5 h. The kinetic experiments were repeated three times for which the averaged data were used.

3.7. Reusability Studies

The model substrate used was benzyl alcohol. The first cycle follows the general procedures for Cu-catalyzed alcohol oxidation (*vide supra*). After 3 h, 500 μL of the reaction mixture was sampled and filtered through silica. The resulting filtrate was used in determining the product yield *via* GC-MS with anisole (0.20 mmol) added as an internal standard. Then, more benzyl alcohol (2.0 mmol) and TEMPO (0.10 mmol) were added into the remaining reaction mixture. After 3 h, the percent conversions were obtained using GC-MS methods using the same workup procedure. Additions of benzyl alcohol and TEMPO followed by GC-MS measurements to determine percent conversions were repeated for five cycles.

Conclusions

We have reported the synthesis of Cu(II) complexes of the type $Cu(NN')_2(OTf)_2$, [NN' = NN'_{Ph} (**1**), NN'_{hex} (**2**), NN'_{py} (**3**), and bpy (**4**)]. For the pyridyl-substituted NN'_{py} ligand, the crystal structure reveals an exclusive binding of Cu(II) ion to the pyridine N and the proximal triazole N donor (*i.e.*, regular-type triazole ligand). Results from CV data and DFT calculations also indicate that the regular triazole ligand (NN'_{py}) is a more electron-rich and better σ-donating ligand, compared to the inverse-type ligands (NN'_{Ph} and NN'_{hex}). On the other hand, based on reduction potentials, the substituents on the triazole ring do not exert much effect on the electron-donating strength of the ligand. The systems Cu^{II}/NN'/Cu^0 in the presence of the TEMPO radical and NMI have been shown as stable and efficient catalysts for aerobic alcohol oxidation, both with aromatic and unhindered aliphatic alcohol substrate. Catalytic studies reveal that rates of activated benzyl alcohol oxidation depend on the ligand electron-donating strength. More specifically, the Cu^{II}/NN'/Cu^0 systems are more active oxidation catalysts in the presence of the more electron-rich N-based ligands.

Acknowledgements

The authors are grateful to Kasempong Srisawad for a technical assistance in the recording of CV data. We acknowledge financial supports from the Thailand Research Fund and Commission on Higher Education for financial support under Grant No. RSA5780058. This work is also supported by the Center of Excellence for Innovation in Chemistry (PERCH-CIC) and Faculty of Science, Mahidol University and Mahidol University under the National Research Universities Initiative.

References

1. M. Hudlicky, *Oxidations in Organic Chemistry*, American Chemical Society, Washington, D.C., 1990.
2. G. Tojo and M. Fernández, *Oxidation of Alcohols to Aldehydes and Ketones*, Springer, New York, 2010.
3. J. R. Holum, *J. Org. Chem.*, 1961, **26**, 4814-4816.
4. K. Omura and D. Swern, *Tetrahedron*, 1978, **34**, 1651-1660.
5. D. B. Dess and J. C. Martin, *J. Org. Chem.*, 1983, **48**, 4155-4156.
6. A. E. J. de Nooy, A. C. Besemer and H. van Bekkum, *Synthesis*, 1996, 1153-1174.
7. T. Punniyamurthy, S. Velusamy and J. Iqbal, *Chem. Rev.*, 2005, **105**, 2329-2364.
8. I. Bento, L. O. Marins, G. G. Lopes, M. A. Carrondo and P. F. Lindley, *Dalton Trans.*, 2005, 3507-3513.
9. J. E. Coleman, *Journal*, 2009, **136**, 267-304.
10. B. K. Santra, P. A. N. Reddy, M. Nethaji and A. R. Chakravarty, *Inorg. Chem.*, 2002, **41**, 1328-1332.

11. M. F. Semmelhack, C. R. Schmid, D. A. Cortés and C. S. Chou, *J. Am. Chem. Soc.*, 1984, **106**, 3374-3376.
12. I. E. Markó, P. R. Giles, M. Tsukazaki, I. Chellé-Regnaut, A. Gautier, S. M. Brown and C. J. Urch, *J. Org. Chem.*, 1999, **64**, 2433-2439.
13. I. E. Markó, P. R. Giles, M. Tsukazaki, S. M. Brown and C. J. Urch, *Science*, 1999, **274**, 2044-2046.
14. P. Gamez, I. W. C. E. Arends, J. Reedijk and R. A. Sheldon, *Chem. Commun.*, 2003, 2414-2415.
15. E. T. T. Kumpulainen and A. M. P. Koskinen, *Chem.-Eur. J.*, 2009, **15**, 10901-10911.
16. J. M. Hoover, B. L. Ryland and S. S. Stahl, *J. Am. Chem. Soc.*, 2013, **135**, 2357-2367.
17. J. M. Hoover, B. L. Ryland and S. S. Stahl, *ACS Catal.*, 2013, **3**, 2599-2605.
18. J. M. Hoover and S. S. Stahl, *J. Am. Chem. Soc.*, 2011, **133**, 16901-16910.
19. D. E. Bergbreiter, P. N. Hamilton and N. M. Koshti, *J. Am. Chem. Soc.*, 2007, **129**, 10666-10667.
20. M. Juríček, P. H. J. Kouwer and A. E. Rowan, *Chem. Commun.*, 2011, **47**, 8740-8749.
21. S. Özçubukçu, E. Ozkal, C. Jimeno and M. A. Pericàs, *Org. Lett.*, 2009, **11**, 4680-4683.
22. P. Sangtrirutnugul, P. Maisopa, L. Chaicharoenwimolkul, A. Sunsin, E. Somsook and V. Reutrakul, *J. Appl. Polym. Sci.*, 2013, **127**, 2757-2763.
23. P. Sangtrirutnugul, K. Wised, P. Maisopa, N. Trongsiriwat, P. Tangboriboonrat and V. Reutrakul, *Polym. Int.*, 2014, **63**, 1869-1874.
24. S. Jindabot, K. Teerachanan, P. Thongkam, S. Kiatisevi, T. Khamnaen, P. Phiriyawirut, S. Charoenchaidet, T. Sooksimuang, P. Kongsaeree and P. Sangtrirutnugul, *J. Organomet. Chem.*, 2014, **750**, 35-40.
25. D. Liu, W. Gao, Q. Dai and X. Zhang, *Org. Lett.*, 2005, **7**, 4907-4910.
26. D. Wang, D. Denux, J. Ruiz and D. Astruc, *Adv. Synth. Catal.*, 2013, **355**, 129-142.
27. E. Hao, Z. Wang, L. Jiao and S. Wang, *Dalton Trans.*, 2010, **39**, 2660-2666.
28. W. Yan, X. Ye, N. G. Akhmedov, J. L. Petersen and X. Shi, *Org. Lett.*, 2012, **14**, 2358-2361.
29. B. Schulze, C. Friebe, M. D. Hager, A. Winter, R. Hoogenboom, H. Görls and U. S. Schubert, *Dalton Trans.*, 2009, 787-794.
30. P. M. Guha, H. Phan, J. S. Kinyon, W. S. Brotherton, K. Sreenath, T. J. Simmons, Z. Wang, R. J. Clark, N. S. Dalal, M. Shatruk and L. Zhu, *Inorg. Chem.*, 2012, **51**, 3465-3477.
31. D. Schweinfurth, C.-Y. Su, S.-C. Wei, P. Braunstein and B. Sarkar, *Dalton Trans.*, 2012, **41**, 12984-12990.
32. T. Romero, R. A. Orenes, A. Espinosa, A. Tárraga and P. Molina, *Inorg. Chem.*, 2011, **50**, 8214-8224.
33. K. J. Kilpin, E. L. Gavey, C. J. McAdam, C. B. Anderson, S. J. Lind, C. C. Keep, K. C. Gordon and J. D. Crowley, *Inorg. Chem.*, 2011, **50**, 6334-6346.
34. W. K. C. Lo, G. S. Huff, J. R. Cubanski, A. D. W. Kennedy, C. J. McAdam, D. A. McMorran, K. C. Gordon and J. D. Crowley, *Inorg. Chem.*, 2015, **54**, 1572-1587.
35. U. Ray, D. Banerjee, G. Mostafa, T.-H. Lu and C. Sinha, *New J. Chem.*, 2004, **28**, 1437-1442.
36. B. Sarkar, S. Konar, C. J. Gómex-García and A. Ghosh, *Inorg. Chem.*, 2008, **47**, 11611-11619.
37. A.-J. DiMaio, A. L. Rheingold, T. T. Chin, D. T. Pierce and W. E. Geiger, *Organometallics*, 1998, **17**, 1169-1176.
38. H. van der Salm, A. B. S. Elliott and K. C. Gordon, *Coord. Chem. Rev.*, 2015, **282-283**, 33-49.
39. M. Munakata, S. Kitagawa, A. Asahara and H. Masuda, *Bull. Chem. Soc. Jpn.*, 1987, **60**, 1927-1929.
40. P. C. Healy, L. M. Engelhardt, V. A. Patrick and A. H. White, *J. Chem. Soc., Dalton Trans.*, 1985, 2541-2545.
41. J. E. Steves and S. S. Stahl, *J. Am. Chem. Soc.*, 2013, **135**, 15742-15745.
42. P. Lahtinen, H. Korpi, E. Haavisto, M. Leskela and T. Repo, *J. Comb. Chem.*, 2004, **6**, 967-973.
43. G. M. Sheldrick, *Acta Cryst.*, 2008, **A64**, 112-122.
44. O. V. Dolomanov, L. J. Bourhis, R. J. Gildea, J. A. K. Howard and H. Puschmann, *J. Appl. Cryst.*, 2009, 339-341.
45. A. Altomare, M. C. Burla, M. Camalli, G. L. Cascarano, C. Giacovazzo, A. Gaugliardi, A. G. G. Moliterni, G. Polidori and R. Spagna, *J. Appl. Cryst.*, 1999, **32**, 115-119.
46. G. M. Sheldrick, *Journal*.
47. M. J. Frisch, G. Trucks, H. Schlegel, G. Scuseria, M. Robb, J. Cheeseman, G. Scalmani, V. Barone, B. Mennucci, G. A. Petersson, H. Nakatsuji, C. M., X. Li, H. P. Hratchian, A. F. Izmaylov, J. Bloino, G. Zheng, J. L. Sonnenberg, M. Hada, M. Ehara, K. Toyota, R. Fukuda, J. Hasegawa, M. Ishida, T. Nakajima, Y. Honda, O. Kitao, H. Nakai, T. Vreven, J. A. Montgomery, Jr., J. E. Peralta, F. Ogliaro, M. Bearpark, J. J. Heyd, E. Brothers, K. N. Kudin, V. N. Staroverov, T. Keith, R. Kobayashi, J. Normand, K. Raghavachari, A. Rendell, J. C. Burant, S. S. Iyengar, J. Tomasi, M. Cossi, N. Rega, J. M. Millam, M. Klene, J. E. Knox, J. B. Cross, V. Bakken, C. Adamo, J. Jaramillo, R. Gomperts, R. E. Stratmann, O. Yazyev, A. J. Austin, R. Cammi, C. Pomelli, J. W. Ochterski, R. L. Martin, K. Morokuma, V. G. Zakrzewski, G. A. Voth, P. Salvador, J. J. Dannenberg, S. Dapprich, A. D. Daniels, O. Farkas, J. B. Foresman, J. V. Ortiz, J. Cioslowski and D. J. Fox, *Journal*, 2010.
48. A. D. Becke, *J Chem Pys*, 1993, **98**, 5648-5652.
49. C. Lee, W. Yang and R. G. Parr, *Phys. Rev. B*, 1988, **37**, 785-789.
50. P. J. Stephens, F. J. Devlin, C. F. Chabalowski and M. J. Frisch, *J. Phys. Chem.*, 1994, **98**, 11623-11627.
51. A. Bergner, M. Dolg, W. Küchle, H. Stoll and H. Preuß, *Mol. Phys.*, 1993, **80**, 1431-1441.
52. P. C. Hariharan and J. A. Pople, *Theoret. Chim. Acta*, 1973, **28**, 213-222.
53. G. A. Petersson and M. A. Al-Laham, *J. Chem. Phys.*, 1991, **94**, 6081-6090.
54. G. A. Petersson, A. Bennett, T. G. Tensfeldt, M. A. Al-Laham, W. A. Shirley and J. Mantzaris, *J. Chem. Phys.*, 1988, **89**, 2193-2218.
55. B. E. Bursten, J. R. Jensen and R. F. Fenske, *J. Chem. Phys.*, 1978, **68**, 3320-3321.
56. M. B. Hall and R. F. Fenske, *Inorg. Chem.*, 1972, **11**, 768-779.
57. J. Manson, C. E. Webster, L. M. Pérez and M. B. Hall, http://www.chem.tamu.edu/jimp2.